



# SHORTEST-PATH-FINDER ALGORITHM IN A TWO-DIMENSIONAL ARRAY OF NONLINEAR ELECTRONIC CIRCUITS

ALBERTO P. MUÑUZURI\* and LEON O. CHUA  
*NOEL, Department of Electrical Engineering and Computer Sciences,  
University of California at Berkeley, Berkeley, CA 94720, USA*

Received May 10, 1997; Revised April 2, 1998

A two-dimensional array of diffusively-coupled nonlinear electronic circuits, Chua's cells, operating in a bistable regime, is used to find the shortest path connecting two points of a given image. Images are previously stored in the system by modulating the diffusion coefficients. Different types of images were considered, from black and white pictures (where 0 means no propagation and 1 propagation), to analog figures (with many intermediate states) and, in all cases, the algorithm used for such calculations succeeded to find the shortest path. The full description of the algorithm is here described and applied to nontrivial cases where the shortest path strongly differs from the straight line.

## 1. Introduction

Autowaves represent a particular class of nonlinear waves that propagate through active media at the expense of the energy stored in the medium and are manifestations of a strongly nonlinear active media [Murray, 1989]. Typical examples of autowaves include the combustion waves, waves of phase transitions, concentrational waves in chemical reactions [Zaikin & Zhabotinsky, 1970; Zhabotinsky & Zaikin, 1973; Zhabotinsky, 1964; Pérez-Muñuzuri *et al.*, 1991; Müller *et al.*, 1987; Jakubith *et al.*, 1990], and many biological autowave processes: Propagation of nerve pulses [Scott, 1975], excitation waves in the cardiac muscle [Allesie *et al.*, 1973, 1977], cultures of the slime mold *Dyctiostelium discoideum* [Cohen & Robertson, 1971], epidemic waves in ecological communities [Capasso & Paveri-Fontana, 1979; Anderson & May, 1986; Kermack & McKendrick, 1933], retina

[Bures *et al.*, 1984], spreading waves in the cerebral cortex [Ermentrout & Cowan, 1979], etc.

On the basis of the fundamental properties of autowaves, it has been possible to use them for some image processing operations [Krinsky *et al.*, 1991; Kuhnert *et al.*, 1989; Mikhailov, 1989; Pérez-Muñuzuri *et al.*, 1993, Steinbock *et al.*, 1995]. In [Pérez-Muñuzuri *et al.*, 1993], the authors demonstrate the possibility of finding the shortest path connecting two points by means of autowave processes. Until now, all the experiments were performed for almost trivial cases where the shortest path corresponds with a slight deviation from the straight line. In this paper, we demonstrate the robustness of autowaves by generalizing these methods to nontrivial cases where the shortest path is a curve completely different from the straight line.

For the purposes of this study, we considered a two-dimensional array of diffusively coupled

---

\*Corresponding author.

Group of Nonlinear Physics. Fac. de Físicas. Univ. de Santiago de Compostela. 15706 Santiago de Compostela. Spain.  
E-mail: munuzuri@fred.eecs.berkeley.edu

nonlinear electronic circuits. The basic cell at the nodes of the array was considered to be a Chua circuit [Chua *et al.*, 1986; Chua, 1992; Madan, 1993]. This circuit has been proven to recover most of the properties of the autowaves [Muñuzuri *et al.*, 1993, 1995; Pérez-Muñuzuri *et al.*, 1995] as well as used to understand the dynamics underlying biological processes (propagation of cardiac pulse [Muñuzuri *et al.*, 1996a, 1996b]) or for image processing in general. It also offers the possibility of direct implementation of these methods via VLSI technology.

In Sec. 2, we present a brief description of the Chua's cell used along this paper as well as the full description of the algorithm used to find the shortest path joining two points. In Secs. 3 and 4, the algorithm will be applied to two nontrivial cases; namely, to a so called binary labyrinth (also called flat labyrinth in literature [Pérez-Muñuzuri *et al.*, 1993]) that either allows the propagation of autowaves or inhibits it completely and to an analog labyrinth (also called wrinkled labyrinth in literature [Pérez-Muñuzuri *et al.*, 1993]) that introduces a scaled difficulty to the propagation of autowaves proportional to some parameter characteristic of the labyrinth (as, for instance, the distance to a ground level). In both cases, the algorithm succeeded to find the shortest path. In Sec. 5, a brief discussion is presented.

## 2. Methods

### 2.1. Chua's circuit

The basic unit of our two-dimensional CNN array is a Chua's circuit [Madan, 1993]. The circuit contains three linear energy-storage elements (an inductor and two capacitors), a linear conductance and a single nonlinear active resistor (Chua's diode). Each cell is coupled to its four adjacent neighbors through linear resistors, thereby simulating a diffusion process. The dynamics of each cell can be described by a third-order autonomous nonlinear differential equation. In particular, we consider the dimensionless form of these equations [Muñuzuri *et al.*, 1995; Pérez-Muñuzuri *et al.*, 1995],

$$\begin{aligned} \frac{du_{i,j}}{dt} &= \alpha[v_{i,j} - h(u_{i,j})] + D_{i,j}(u_{i+1,j} + u_{i-1,j} \\ &\quad + u_{i,j+1} + u_{i,j-1} - 4u_{i,j}) \\ \frac{dv_{i,j}}{dt} &= u_{i,j} - v_{i,j} + w_{i,j} \\ \frac{dw_{i,j}}{dt} &= -\beta v_{i,j} - \gamma w_{i,j} \end{aligned} \quad (1)$$

with  $i = 1, \dots, N$ ,  $j = 1, \dots, M$  and  $N \times M$  is the size of the medium. The function  $h(u_{i,j})$  describes the three-segment piecewise-linear curve of the nonlinear resistor given by,

$$h(u_{i,j}) = \begin{cases} \varepsilon + m_1 u_{i,j} - (m_0 - m_1) & u_{i,j} \leq x_1 \\ \varepsilon + m_0 u_{i,j} & x_1 < u_{i,j} \leq x_2 \\ \varepsilon + m_2 u_{i,j} + (m_0 - m_2) & u_{i,j} > x_2 \end{cases} \quad (2)$$

where  $\alpha$ ,  $\beta$  and  $\gamma$  are the parameters of the system related with the characteristic physical quantities of the circuit by:  $\alpha = C_2/C_1$ ,  $\beta = C_2/(LG^2)$  and  $\gamma = (C_2 r_o)/(LG)$ .  $m_0$ ,  $m_1$  and  $m_2$  are parameters responsible for the nonlinear resistor and  $\varepsilon$  is a small constant called "dc offset".  $D_{i,j}$  plays the role of a diffusion coefficient and takes into account the influence of the neighboring cells through the coupling resistors ( $D_{i,j} = \alpha/(GR)$ ) and for the purposes of this paper we considered it to be dependent on the cell.

The set of parameters used along this paper are:  $\alpha = 9$ ,  $\beta = 30$ ,  $\gamma = 0$ ,  $m_0 = -0.14$ ,  $m_1 = m_2 = 0.14$ ,  $\varepsilon = -0.1$  and  $D_{i,j}$  was different depending on the case.

### 2.2. Labyrinth implementation

A labyrinth is implemented in the system by modulating the diffusion coefficient,  $D_{i,j}$ , of each cell. For the case of a binary labyrinth, as the one considered in Sec. 3, we take  $D_{i,j} = DI_{i,j}$ , where  $I_{i,j}$  is the image considered.  $I_{i,j}$  is a binary image with  $I_{i,j} = 0$  for those points where no wave propagation is expected and  $I_{i,j} = 1$  for normal propagation. The values of  $I_{i,j}$  are kept unchanged along the experiment.

In Sec. 4 an analog labyrinth is considered. There, the image  $I_{i,j}$  is composed of real numbers between 0 and 1. 0 means no propagation, 1 normal propagation or maximum velocity propagation and any intermediate value reflects the difficulty to propagate through the medium.

The image,  $I_{i,j}$ , can be used to introduce in the system different factors (or a combination of several of them) that may change the solution to the shortest path problem.

### 2.3. Path-finder algorithm

Several algorithms have been so far developed to find the shortest path between two points [Dantzig,

1951; Ford & Fulkerson, 1956; Lee, 1961; Moore, 1959; Prim, 1957; Pérez-Muñuzuri *et al.*, 1993] and their applicability studied. But, as far as we know, the experiments have been done only for trivial cases where the shortest path just differs slightly from the straight line. The examples considered in this paper are taken from real problems and the algorithm described below resulted successful in all the cases considered.

For the choice of parameters considered in this paper, the system is guaranteed to have two stable equilibrium points,  $P_+$  and  $P_-$  for each cell. Due to the asymmetry of function  $h(u)$ , the basin of attraction of one of the points,  $P_+$ , is larger than the other,  $P_-$ . This allows, in an extended system as ours, the propagation of a traveling wave [Muñuzuri *et al.*, 1995].

Once a traveling wave is created, it propagates in all allowed directions with constant velocity “exploring” all possible paths. Because of the constant velocity of the waves, the shortest path will coincide with the path that takes the least time to be covered.

The numerical algorithm used in the simulations here presented can be summarized as follows:

- (a) The whole system is set to the equilibrium state  $P_-$ . A square of  $3 \times 3$  cells, centered around the starting point  $P_1$ , are triggered out to the more stable equilibrium point  $P_+$ , thus, initiating a traveling wave that will finally cover the whole medium.
- (b) As the different fronts of the wave propagate (in the case of a complicate maze), the times when each cell is triggered out from the state  $P_-$  to the state  $P_+$  are recorded. This process lasts until the target point,  $P_2$ , is reached for the first time (in this way we have measured the minimum time needed to reach the final destination,  $t_{\text{tot}}$ ).
- (c) At this point, the shortest path is rebuilt, starting from the final point ( $P_2$ ), by using the previously stored data in the following way. The total time invested to reach  $P_2$ ,  $t_{\text{tot}}$ , is divided in a large number of time steps (each one lasting  $t_{\text{step}}$ ). The next point of the shortest path is chosen as the closest to  $P_2$  that was excited during the time interval  $[t_{\text{tot}} - t_{\text{step}}, t_{\text{tot}}]$ . The next point of the shortest path is, then, chosen as the closest to the previous that was excited during the time interval  $[t_{\text{tot}} - 2t_{\text{step}}, t_{\text{tot}} - t_{\text{step}}]$ .

This process is repeated for all possible times (until  $t = 0$ ) and the desired shortest path is recovered.

This algorithm can be applied to both types of labyrinths considered in this paper, binary and analog. The use of autowaves for this image processing operation results in a very high degree of parallelism since all the elements of the medium evolve simultaneously.

### 3. Binary Labyrinth

In this section, we stored in the system a binary image as described in Sec. 2. We considered a maze taken from a garden in England [Fisher, 1990].

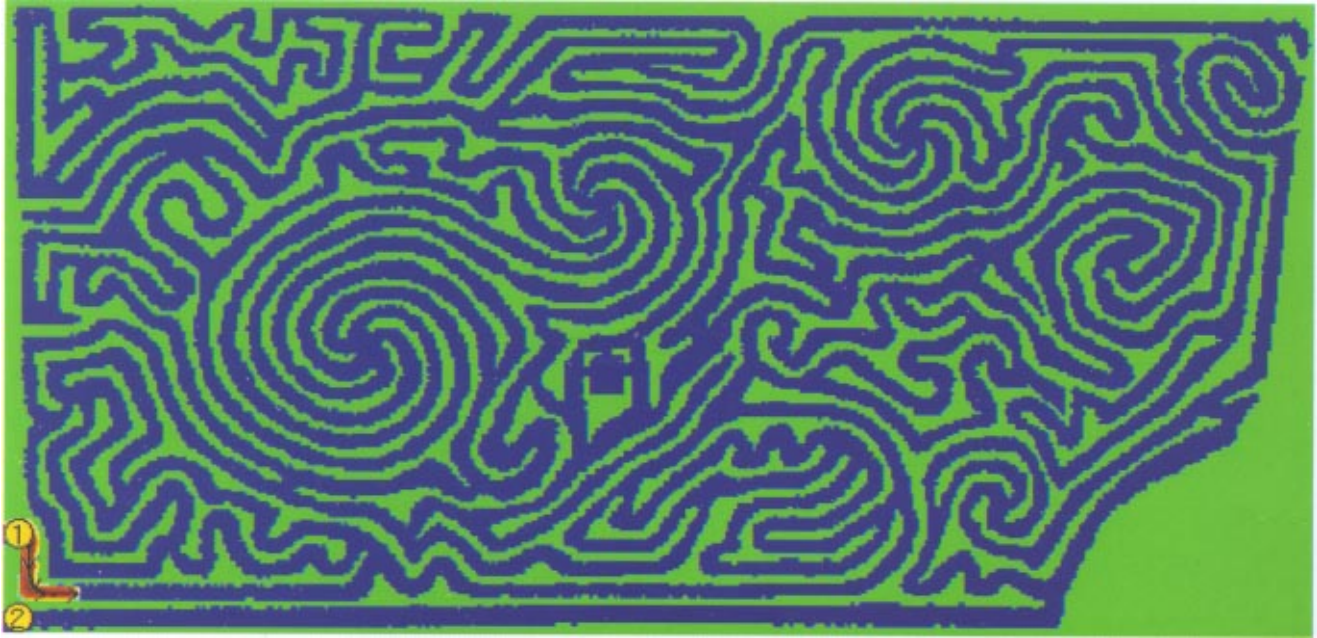
Figure 1(a) shows the binary labyrinth as well as the state of the system at time  $t = 60$  t.u. after the beginning of the experiment. Green color marks the points of no propagation, red denotes the points in the more stable state,  $P_+$ , and blue points in the state  $P_-$ . The starting point,  $P_1$ , where the traveling wave was triggered out is marked with the number 1 surrounded by a yellow spot. The final destination,  $P_2$ , is marked by the number 2 in the figure. The black line with arrows shows the part of the shortest path already covered (calculated as described in Sec. 2).

As time evolves, the traveling wave propagates through all possible paths with constant velocity [Figs. 1(b) and 1(c)], thus, checking all possible solutions of the system. The optimal path is obtained when the traveling wave first reaches the final point,  $P_2$  [Fig. 1(d),  $t = 3140$  t.u.).

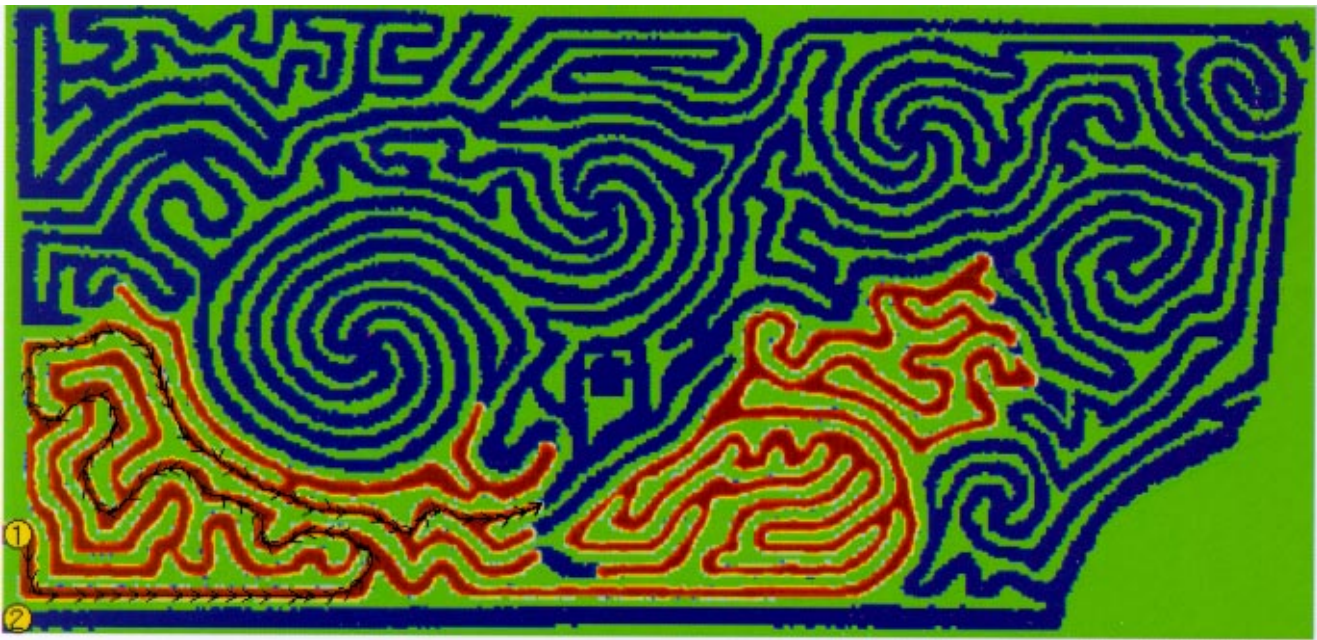
### 4. Analog Labyrinth

In this section, an analog labyrinth is considered to be stored in the system as described in Sec. 2. In this case, a topographic map from the area of San Francisco in North California was considered. This constitutes a much more complicate case than the previous one as unpenetrable obstacles (such as coast lines, lakes, etc.) are considered as well as difficulties to the wave propagation (such as mountains) that actually slow down the velocity of the traveling wave. Now, the image,  $I_{i,j}$ , is composed of points with 0 value, representing impenetrable obstacles, 1 for areas of highest velocity and intermediate values for mountain regions.

Figure 2(a) shows the map considered as well as the overlapped state of the system at  $t = 40$  t.u.

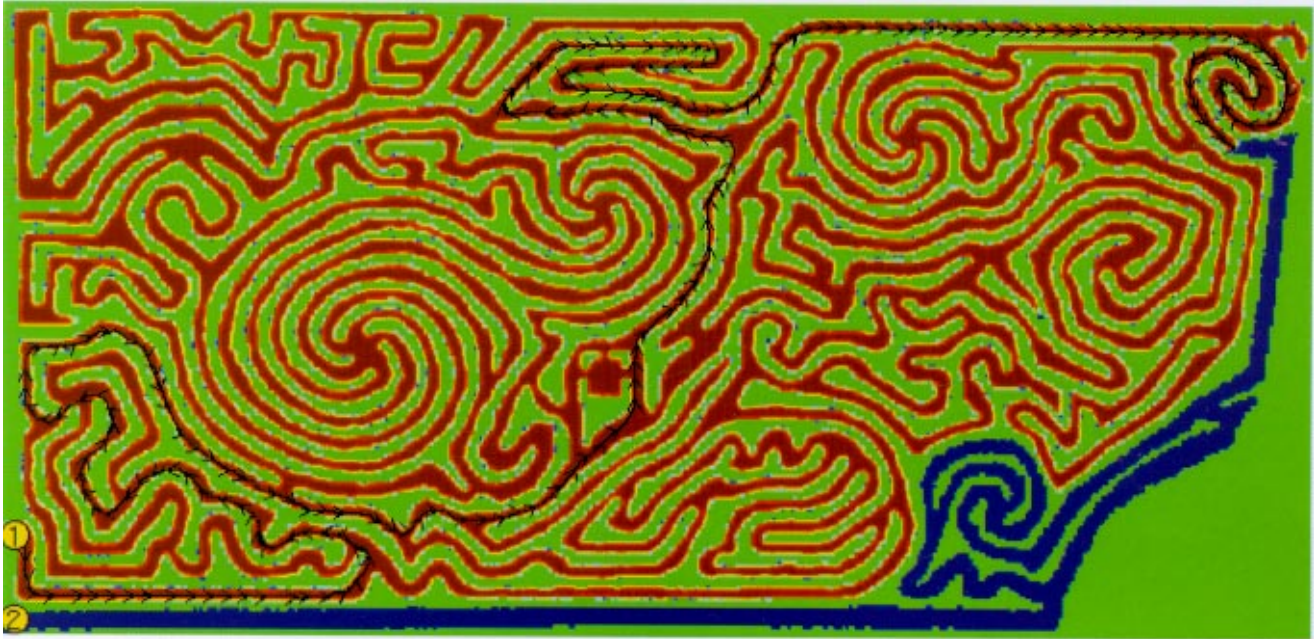


(a)

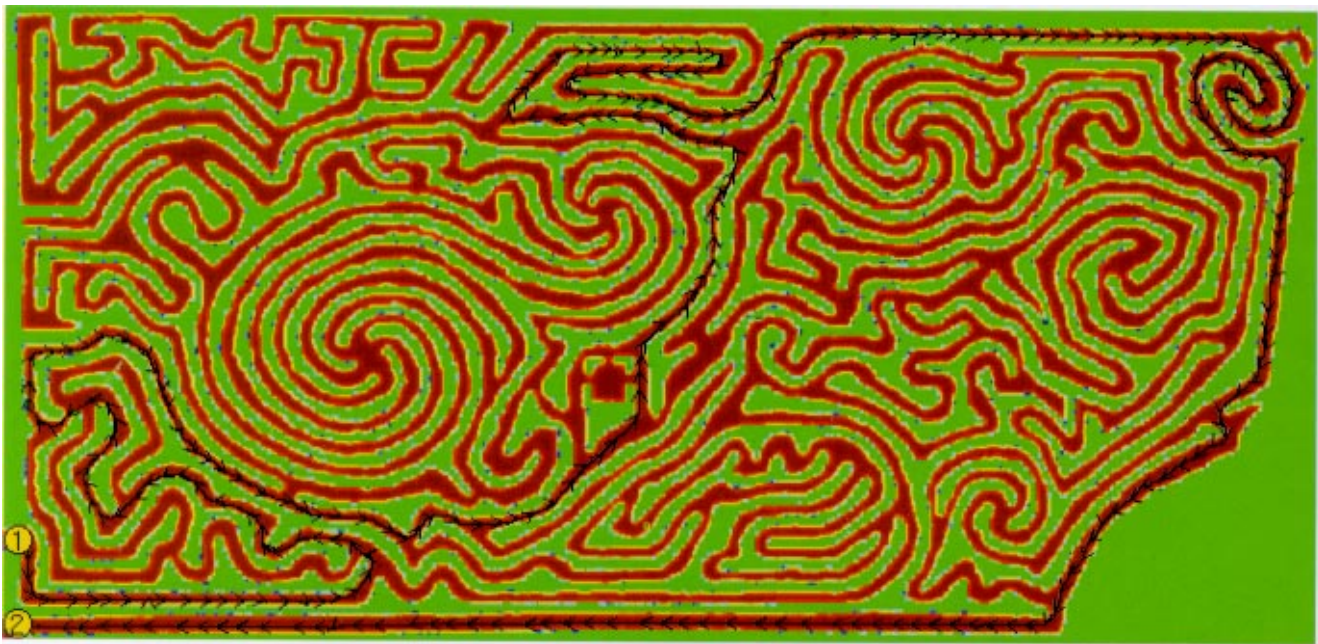


(b)

Fig. 1. Binary labyrinth. The different snapshots show the evolution of the traveling waves through the system: (a)  $t = 60$  t.u., (b)  $t = 940$  t.u., (c)  $t = 2260$  t.u. and (d)  $t = 3140$  t.u. The starting point,  $P_1$ , where the traveling wave was triggered out is marked with the number 1 surrounded by a yellow spot and the final destination,  $P_2$ , by the number 2. Green color marks the points of no propagation, red denotes the points in the more stable state,  $P_+$ , and blue points in the state  $P_-$ . The black line with arrows shows the part of the shortest path already covered. ( $D = 1$ , image size  $851 \times 411$  cells.)



(c)



(d)

Fig. 1. (Continued)

after the beginning of the simulation. Blue color marks areas of impenetrable obstacles (such as sea, lakes, etc; rivers are considered to be penetrable). Red is used to mark points in the more stable state,  $P_+$ , the rest of the points (in the state  $P_-$ ) are depicted with the colors from the original map that represent different heights from the sea level. The

initial and final points are, like in the previous example, marked with the numbers 1 and 2. The black line with arrows shows the part of the shortest path already covered.

In Figs. 2(b) and 2(c), the traveling wave propagates through the medium checking all possible paths. Notice that some parts in the figure are not

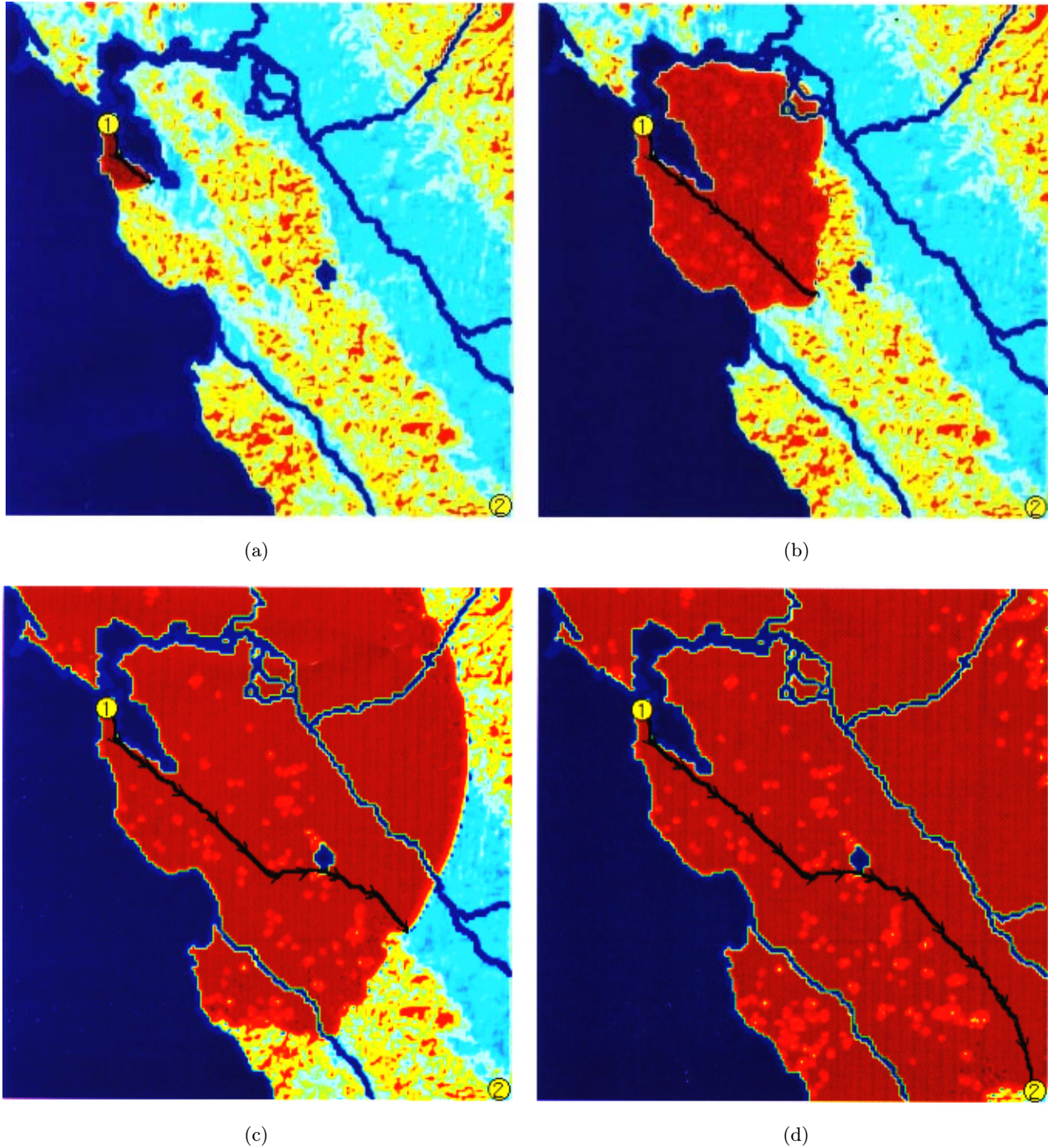


Fig. 2. Analog Labyrinth. The different snapshots show the evolution of the traveling waves through the system: (a)  $t = 40$  t.u., (b)  $t = 120$  t.u., (c)  $t = 2000$  t.u. and (d)  $t = 280$  t.u. The starting point,  $P_1$ , where the traveling wave was triggered out is marked with the number 1 surrounded by a yellow spot and the final destination,  $P_2$ , by the number 2. Blue color marks areas of impenetrable obstacles (such as sea, lakes, etc, rivers are considered to be penetrable). Red is used to mark points in the more stable state,  $P_+$ , the rest of the points (in the state  $P_-$ ) are depicted with the colors from the original map that represent different heights from the sea level. The black line with arrows shows the part of the shortest path already covered. ( $D = 2$ , image size  $337 \times 339$  cells.)

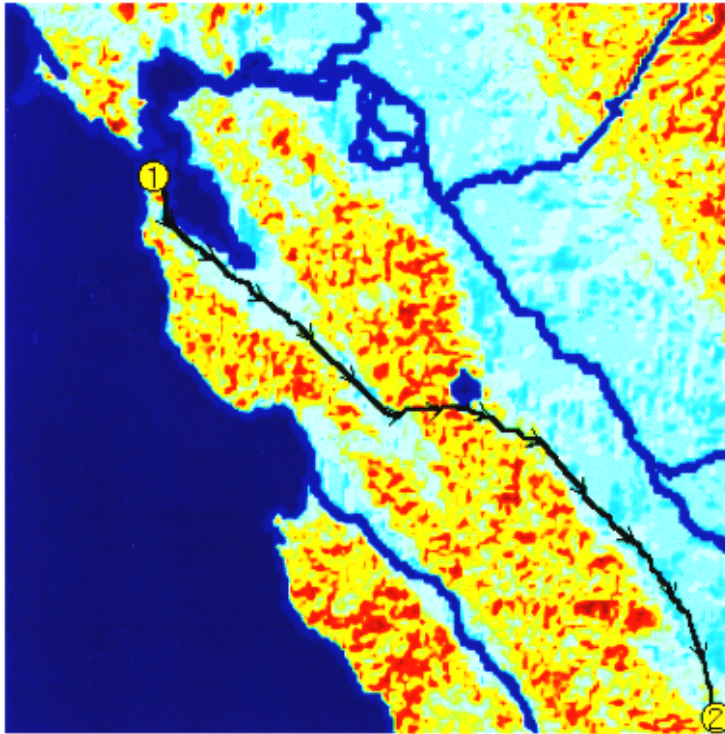


Fig. 3. Map of the area considered for simulations as well as the calculated shortest path. Different colors represent different heights from the sea level (blue is the sea level and red is the highest point). (Same parameters as in Fig. 2.)

in red after the wave went over, these parts correspond with large heights and equivalently with small diffusion coefficients, smaller than the minimum required to have wave propagation [Pérez-Muñuzuri *et al.*, 1992].

The final state is shown in Fig. 2(d) at  $t = 280$  t.u. The traveling wave already reached the final point,  $P_2$ , and the shortest path is obtained. In Fig. 3, the map of the area considered (without the traveling wave) is depicted as well as the shortest path (black line with arrows) obtained during the simulations.

## 5. Conclusions

In this paper, we demonstrated the robustness of the autowaves to find the shortest path in a nonhomogeneous medium. Even in the most complicated cases, as those here described, the shortest path was obtained. Also, the detailed algorithm used for the simulations is explained along the text.

This system also offers the possibility to include other factors that can be easily implemented, i.e. shortcuts or a combination of different factors. It is also possible to encode information about the

slope of the path, i.e. for positive slopes the velocity is decreased and vice versa.

The nature of the system considered, a two-dimensional array of Chua's cells, allows the exact control of each single parameter in the medium, thus, more complicate obstacles or topographies can be implemented by just defining some potential energy map that can be considered as the image,  $I_{i,j}$ . The basic discrete nature of the described system allows to build up three-dimensional systems (or systems of higher dimensionality where each dimension does not correspond necessarily with a spatial axis) where the shortest path is a curve in the three-dimensional space considered.

Another point checked was the advantage of working in a bistable regime rather than in a monostable regime. In the first case, a transition wave from state  $P_-$  to  $P_+$  propagates through the medium, finally being the whole medium in  $P_+$ . Meanwhile, in the second case, as the wave propagates, points in the medium are temporally triggered out from the equilibrium state. This allows to re-excite the points of the medium several times, thus, leading to a more complicate situation where several frontwaves can propagate in the same direction. Also curvature effects at the edges of the

obstacles may induce the appearance of spiral waves in the system [Gómez-Gesteira, 1994] (that will continuously send waves in all directions). Now, the final state is not homogeneous but the picture is rather more complicated with several waves propagating through the medium. Thus, traveling waves constitute the best choice for this kind of image processing analysis.

## Acknowledgments

A. P. Muñuzuri acknowledges Dr. V. Pérez-Muñuzuri for helpful discussions. Calculations were performed at the *Centro de Supercomputación de Galicia (CESGA)*, Spain.

## References

- Allesie, M. A., Bonke, F. I. M. & Scopman, T. Y. G. [1973] "Circus movement in rabbit atrial muscle as a mechanism in tachycardia," *Circ. Res.* **33**, 54–62.
- Allesie, M. A., Bonke, F. I. M. & Schopman, F. G. J. [1977] "Circus movement in rabbit atrial muscle as a mechanism of tachycardia. III. The 'leading circle' concept: A new model of circus movement in cardiac tissue without the involvement of an anatomical obstacle," *Circ. Res.* **41**, 9–18.
- Anderson, R. M. & May, R. M. [1986] "The invasion, persistence and spread of infectious diseases within animal and plant communities," *Phil. Trans. R. Soc. London* **B314**, 533–570.
- Bures, J., Koroleva, V. I. & Gorelova, N. A. [1984] "Leao's spreading depression, an example of diffusion-mediated propagation of excitation in the central nervous system," *Autowaves and Structures Far from Equilibrium*, ed. Krinsky, V. I. (Springer-Verlag), pp. 180–183.
- Capasso, V. & Paveri-Fontana, S. L. [1979] "A mathematical model for the 1973 cholera epidemic in the European Mediterranean region," *Rev. Epidém. et Santé Publ.* **27**, 121–132.
- Chua, L. O., Komuro, M. & Matsumoto, T. [1986] "The double-scroll family, Parts I and II," *IEEE Trans. Circuits Syst.* **33**, 1073–1118.
- Chua, L. O. [1992] "The genesis of Chua's circuits," *Int. J. Elec. Commun.* **46**, 250–257.
- Cohen, M. M. & Robezton, A. [1971] "Chemotaxis and early stages of aggregation in cellular slime molds," *J. Theor. Biol.* **31**, 119–130.
- Dantzig, G. B. [1951] "Maximization of a linear function of variables subject to linear inequalities," Cowles Commission.
- Ermentrout, G. B. & Cowan, J. [1979] "A mathematical theory of visual hallucination patterns," *Biol. Cybern.* **34**, 137–150.
- Fisher, A. [1990] *Labyrinth: Solving the Riddle of the Maze* (Harmony Books, NY).
- Ford, L. R. & Fulkerson, D. R. [1956] "Maximal flow through a network," *Can. J. Math.* **8**, 399–404.
- Gómez-Gesteira, M., del Castillo, J. L., Vázquez-Iglesias, M. E., Pérez-Muñuzuri, V. & Pérez-Villar, V. [1994] "Influence of the critical curvature on spiral initiation in an excitable medium," *Phys. Rev.* **E50**(6), 4646–4649.
- Jakubith, S. & Rotermund, H. *et al.* [1990] "Spatiotemporal concentration patterns in a surface reaction: Propagating and standing waves, rotating spirals and turbulence," *Phys. Rev. Lett.* **65**, 3013–3016.
- Kermack, W. O. & McKendrick, A. G. [1933] "Contributions to the mathematical theory of epidemics," *Proc. R. Soc.* **A141**, 94–122.
- Krinsky, V. I., Biktashev, V. N. & Efimov, I. R. [1991] "Autowaves principles for parallel image processing," *Physica* **D49**, 247–253.
- Kuhnert, L., Agladze, K. I. & Krinsky, V. I. [1989] "Image processing using light-sensitive chemical waves," *Nature* **337**, 244–247.
- Lee, C. Y. [1961] "An algorithm for path connections and its applications," *IRE Trans. Electron. Comput.* **EC-10**, 346–365.
- Madan, R. N. (ed.) [1993] *Chua's Circuit: A Paradigm for Chaos*, World Scientific Series on Nonlinear Science, Series B, Vol. 1. (World Scientific, Singapore).
- Mikhailov, A. S. [1989] "Engineering of dynamical systems for pattern recognition and information processing," *Nonlinear Waves 2*, eds. Gaponov-Grekhov, A. V., Rabinovich, M. I. & Engelbrecht, J. (Springer-Verlag, NY), pp. 104–115.
- Moore, E. F. [1959] "Shortest path through a maze," in *Ann. Comput. Lab. of Harvard University* (Harvard University Press, Cambridge, MA) **30**, 285–292.
- Müller, S. C., Plessner, T. & Hess, B. [1987] "Two-dimensional spectrophotometry of spiral wave propagation in the Belousov-Zhabotinsky reaction I. Experiments and digital representation. II. Geometric and kinematic parameters," *Physica* **D24**, 71–96.
- Muñuzuri, A. P., Pérez-Muñuzuri, V., Pérez-Villar, V. & Chua, L. O. [1993] "Spiral waves on a 2D array of nonlinear circuits," *IEEE Trans. Circuits Syst.* **40**, 872–877.
- Muñuzuri, A. P., Pérez-Muñuzuri, V., Gómez-Gesteira, M., Chua, L. O. & Pérez-Villar, V. [1995] "Spatiotemporal structures in discretely-coupled arrays of nonlinear circuits: A review," *Int. J. Bifurcation and Chaos* **5**(1), 17–50.
- Muñuzuri, A. P., deCastro, M., Hofer, E., Pérez-Muñuzuri, V., Gómez-Gesteira, M. & Pérez-Villar, V. [1996a] "Continuous conductive volume affects the propagation of signals in discrete systems," *Int. J. Bifurcation and Chaos* **6**, 1829–1835.
- Muñuzuri, A. P., deCastro, M., Pérez-Muñuzuri, V.,

- Gómez-Gesteira, M., Mariño, I. P., Hofer, E. & Pérez-Villar, V. [1996b] “An electronic real-time model of one-dimensional discontinuous conduction of the cardiac impulse realized with Chua’s circuits,” *Industrial Applications in Power Systems, Computer Science and Telecommunications 4* (IEEE Catalog Number: 96CH35884, ISBN: 0-7803-3109-5).
- Murray, J. D. [1989] *Mathematical Biology* (Springer-Verlag, NY).
- Pérez-Muñuzuri, V., Aliev, R., Vasiev, V., Pérez-Villar, V. & Krinsky, V. I. [1991] “Super-spiral structures in an excitable medium,” *Nature* **353**, 740–742.
- Pérez-Muñuzuri, V., Pérez-Villar, V. & Chua, L. O. [1992] “Propagation failure in linear arrays of Chua’s circuits,” *Int. J. Bifurcation and Chaos* **2**, 403–406.
- Pérez-Muñuzuri, V., Pérez-Villar, V. & Chua, L. O. [1993] “Autowaves for image processing on a two-dimensional CNN array of excitable nonlinear circuits: Flat and wrinkled labyrinths,” *IEEE Trans. Circuits Syst. I* **40**, 174–181.
- Pérez-Muñuzuri, V., Muñuzuri, A. P., Gómez-Gesteira, M., Pérez-Villar, V., Pivka, L. & Chua, L. O. [1995] “Nonlinear waves, patterns and spatio-temporal chaos in cellular neural networks,” *Phil. Trans. R. Soc. London, Series A* **353**, 101–113.
- Prim, R. C. [1957] “Shortest connection networks and some generalizations,” *Bell Syst. Tech. J.* **36**, 1389–1401.
- Scott, A. C. [1975] “The electrophysics of a nerve fiber,” *Rev. Mod. Phys.* **47**, 487–533.
- Steinbock, O., Toth, A. & Showalter, K. [1995] “Navigating complex labyrinths — optimal paths from chemical waves,” *Science* **267**, 868–871.
- Zaikin, A. N. & Zhabotinsky, A. M. [1970] “Concentration wave propagation in two-dimensional liquid phase self-organizing system,” *Nature* **225**, 535–537.
- Zhabotinsky, A. M. [1964] “Periodic processes of the oxidation of malonic acid in solution (Study of the kinetics of Belousov’s reaction),” *Biofizika* **9**, 306–311.
- Zhabotinsky, A. M. & Zaikin, A. N. [1973] “Autowave processes in a distributed chemical system,” *J. Theor. Biol.* **40**, 45–61.